
How Self-Supervised Learning Can be Used for Fine-Grained Head Pose Estimation?

Mahdi Pourmirzaei¹, Gholam Ali Montazer¹, Farzaneh Esmaili¹, Ebrahim Mousavi¹, Sasan Karamizadeh²

{m.poormirzaie, montazer, f.esmaili, e.moosavi}@modares.ac.ir, s.karamizadeh@itrc.ac.ir

Tarbiat Modares University¹, ICT Research Institute²

Abstract

The cost of Head View point labels is the main hurdle in the improving of fine-grained Head Pose estimation algorithm. One solution to the lack of huge number of labels is using Self-Supervised Learning (SSL). SSL can extract good features from unlabeled data for a downstream task. Accordingly, this article has tried to show the difference between SSL approaches for Head Pose estimation. In general, there are two main approaches to use SSL: (1) Using it to pre-train the weights, (2) Leveraging SSL as an auxiliary task besides of Supervised Learning (SL) in one training session. In this paper, we compared two approaches by designing a Hybrid Multi-Task Learning (HMTL) architecture and assessing it with two SSL pre-text tasks, the rotation and puzzling. Results showed that the combination of both methods in which using rotation for pre-training and using puzzling for auxiliary head were the best. Together, the error rate was reduced up to 23.1% compared to the baseline which is comparable with current SOTA methods. Finally, we compared the impact of initial weights on the HMTL and SL. Subsequently, by HMTL, the error was reduced with all kinds of initial weights: random, ImageNet and SSL.

Key-words: Head Pose Estimation, Self-Supervised Learning, Supervised Learning, Multi-Task Learning.

1. Introduction

Facial analysis is considered as one of the most important tasks in computer vision field. This includes such tasks as Face detection, Facial Landmarks detection, Facial Age estimation and Head Pose estimation. To be precise, among them, Head Pose estimation plays a vital role in many practical applications such as driver monitoring [1], human-computer interaction [2], [3], human behavior analysis [4] and Face Recognition [5]. Because in many unconstrained scenarios, they require a Facial Pose estimator which is resistant to environmental variations such as occlusion and illumination [6]. That's why, Head Pose and Facial Pose estimation have gained huge attentions in the past years [6]–[8].

In general, there are mainly two methods exist for Head Pose estimation [9]. To be exact, the first one is based on the Facial Landmarks detection. It means, at first, we have to extract Landmarks from faces and then, after keypoint detection, the Head Pose is calculated from them. Although keypoint detectors

have recently improved substantially due to deep learning boom, Head Pose recovery with this method is fundamentally a two steps process with frequent opportunities for error. For instance, if satisfactory keypoints fail to be detected, then Pose recovery is impossible [7]. The second method is based on the end-to-end learning from images. In other words, the neural network tries to find Head Pose angles from images of faces alone. The data shows that the latter has outperformed landmark-to-pose methods significantly [7], [8], [10]–[12].

Nevertheless, the improvement in the end-to-end learning is usually constrained by the number of labels. The difficulty and time consuming of Head Pose labeling is the main reason for the low amount of datas compared to many computer vision fields. Thus, unlike other computer vision issues, collecting large amounts of labeled data for Head Pose is challenging and may adversely impact on quality of annotating. But, recently, with impressive progress of SSL [13]–[15], unsupervised learning becomes important again, and results show that in an end-to-end learning manner, SSL methods can help us to overcome needing lots of labels. That is to say, SSL is mostly using as a pre-training step nowadays and therefore, common end-to-end methods are using them in order to do fine-tuning on the pre-trained weights. However, those methods have only gotten famous for classification tasks, and for fine-grained problems like Head Pose estimation, they have not been used as they should. We guess, when we do those SSL pre-trainings on Head Pose images, a model at best can learn race or identity features from images and their representation have a little information to detect the position of heads. Also, another problem of current best SSL techniques is needing to the huge amount of data and computations to work well. This means for a domain like Head Pose which resources are quite limited, those approaches are not going to work well. Nonetheless, we think that SSL can be helpful for fine-grained task but in a different setting.

To clarify, in a study [16], it is shown that Self-Supervised pre-text tasks could extract good features for downstream tasks even when it is doing on one image. In fact, when we do pre-training, middle layers show valuable features concerning final layers. Also, by moving from low level layer to high level layer, increase and then decrease could be seen in linear evaluation of their features. From another view, this issue could be looked

through Multi-Task Learning (MTL) settings. Before a certain point, two tasks enhancing shareable features for each other and after that layer, they start hurting each other [17], [18]. It is described as cooperation and competition between tasks. So, this article tried to address SL with auxiliary SS tasks simultaneously in the form of MTL.

In general, there are two main approaches to use SSL: (1) Using pre-trained weights which can be done via SSL tasks, (2) Leveraging SSL as an auxiliary task besides of Supervised Learning (SL) tasks at the same time to help main task which called HMTL [19]. In this paper, we compared the two approaches with jigsaw puzzling and rotation SSL pre-text tasks. Thereafter, we examined the impact of adding auxiliary SSL tasks to the fine-grained Head Pose problem with different settings. We found that our proposed HMTL architecture method acts differently compare to utilizing SSL in the conventional protocol - pre-training and then fine-tuning. In simple words, if we have a supervised task A and a Self-Supervised (SS) task B, there is a difference between results of using B as pre-training, with using B as an auxiliary task besides A. Additionally, we noticed when a SSL pre-training is effective in order to being fine-tuned on Head Pose estimation, it doesn't mean the SSL would also be good to leverage as an auxiliary task besides Head Pose.

All together, we designed a multi-task neural network based on the ResNet50 to couple the SS auxiliary tasks with it. As a matter of fact, we investigated how the representation could be shared to reduce the error rate in the Head Pose estimation head. In addition, we compared the impact of initial weights on the proposed multi-task architecture, HMTL. Subsequently, by HMTL, the error was reduced with all kinds of initializer such as random weights, ImageNet weights and SSL pre-trained weights. Our method was trained on 300W-LP [20] and evaluated on the AFLW2000 [21], BIWI [22] and ETH-XGaze [23] databases. To be exact, the ETH-XGaze was used because it divided pictures based on subjects. The important point about our method is that it can easily pair with other supervised Head Pose methods. Furthermore, although our method, HMTL, showed the lowest error rate when we used both SSL approaches, but it could be quite effective in one training process as well, even without the SSL pre-training stage. In a nutshell, the contributions of this paper are summarized as follows:

1. We searched for the best architecture of HMTL method by using two different kinds of auxiliary SS pre-text tasks besides Supervised Heads (SHs). The two SSL methods were the puzzling and a customized form of the rotation.
2. We showed the effect of SSL pre-training and ImageNet pre-training on both vanilla and multi-task form (HMTL) of the ResNet50 architecture.
3. The difference of HMTL and SL were shown on low data regime with an ablation study.

1.2 Related works

Among several deep learning models, convolutional neural networks (CNNs) are playing vital roles in Pose estimation. Although, Face Pose estimation is a regression problem, since proposing of HopeNet [7], most proposing methods has combined the regression with the classification task. To be

precise, HopeNet utilize multi-task loss functions which consider for each angle. Their proposed loss has two parts, the first one is a pose bin classification and second one is the regression part. Regression values are calculated by expectation of pose classification. They also showed that their model could be generalized for different datasets.

According to the lack of sufficient training data for head pose. In the research [6], they reconstruct the Facial Pose estimation as a label distribution problem which attend each image as an instance affiliated with a Gaussian label distribution rather than a single label, then they build CNN network with muti-loss function.

Furthermore, a work [10] developed a head pose estimation model with two ensembles with top-k regression. The first stage is a binned classification and the second stage, unlike HopeNet, uses the average of top-k classes to find regression values instead of expectation of all bins. Also, they showed that the efficiency of bin classification is dependent on angle distance when using CNNs at the first stage. Moreover, the WHE-Net [11] proposed a loss function for regression tasks. They proposed a method which is convenient for full-range of head yaws or frontal head pose estimation. Afterwards, they created a wrapped loss function to enhance accuracy for anterior views in full-range head pose estimation which properly handles wrapping of yaw. Via their wrapped loss function, instead of penalizing angle straight, it penalizes the minimal rotation angle that is necessary. A work [9] tried to enhance Head Pose by designing a method with two stages. First stage contained a neural network with one regression head and four regression classification head. With using offsets of bounding box, ensemble of offsets was built. Second stage performed knowledge distillation from the ensemble of offsets of the base neural network.

2. Self-Supervised learning

SSL methods are used to learn features from unlabeled data without using annotated labels and it appears with basically three types of approaches:

1. Contrastive learning
2. Non-contrastive learning
3. Pretext task learning

Over the past few years, best SSL methods, gradually moved from pretext task learning like rotation, colorization and jigsaw puzzling to Contrastive learning [24] and the new non-contrastive methods [13], [14], [25]. Even though, recent SSL methods were successful to get better results, but they have some drawbacks which did not solve yet completely, such as huge amount of computation resources and data to work [26], requiring large batch sizes to train because of negative samples [24], and lagging far behind of the supervised learning methods on fine-grained visual classification tasks [26], [27].

As far as we understand, there are only two studies about SSL in the Head view point learning [19], [28]. In a work [28], they propose an analysis-by-synthesis framework for learning viewpoint estimation in a SSL setting by using cycle-consistency losses between a viewpoint estimation and a viewpoint aware synthesis network. Also, a study [19] tried to

combined SSL as auxiliary task besides SL in a MTL manner. They merged Self-Supervised Heads (SSHs) of pre-text tasks with fine-grained Facial Emotion Recognition (FER), Head Pose estimation and Gender recognition tasks. Besides them, the closest research to the Head Pose in which SSL were used, are related to Body Pose [29], [30] and Hand Pose estimation [31].

SSL is not limited to pre-training stage only, some works proposed Self-Supervised co-training to use for Supervised tasks to address disadvantages of pure SSL in visual tasks. In a work [32], they developed a semi-supervised learning framework that benefited the co-training idea using self-supervised techniques for visual representations. This method utilized exemplar and rotation self-supervision techniques as an approach for lack of annotated data, and model performance improved only by using 10% labeled data and 90% unlabeled data. In a study [33], it was found that using cross-modal self-supervision for pre-training is a good idea and could be improved multi-sensory model's performance. They implemented a form of co-training in which the two modalities correlated but had different types of information about the video. In another study [34], they implemented a self-supervised co-training scheme called Co-training Contrastive Learning of visual Representation (CoCLR) that enhanced the infoNCE loss. Furthermore, they showed that hard positives are being ignored in the self-supervised training, and if these hard positives are used, then the quality of learnt representation enhances enormously.

3. Methodology

The procedure of designing an architecture and creating SSL pre-text tasks is described in this section. It needs to be mentioned that in this work, SL+SSL, HMTL and auxiliary SS training are used interchangeably.

3.1 Multi-task architecture

Two architectures were tried in this section: SL, SL + SSL. The first one is exactly the method HopeNet and the second one is based on adding SSL branch to the original HopeNet.

In order to find the best architecture of HMTL, four flag points in ResNet50 [35] to find the best branching point on the main supervised branch for each SS tasks were defined. As ResNet50 has four main blocks and each block includes sub blocks of convolution layers, flag points are defined after main blocks (Fig 1). After finding the best dividing point, we will be able to create the best SL + SSL architecture, based on the ResNet50 architecture.

3.2 SSL tasks for Head Pose estimation

For Head Pose estimation we considered three SSL pre-text tasks:

Puzzling. Like a study [19], some sort of jigsaw puzzling method was used, which performed on an image and moved different part of an image randomly and a neural network model tried to find the correct piece of each region. For each region or part, a classification head would be created. For example, 2×2 puzzling has four SSL heads (Fig 2): $\{H \in \{Region 1, \dots, Region 4\}\}$.

Rotation. Images were rotated by the conventional rotation method [36] at $n*90$ degrees. N is chosen randomly from $\{0, \dots, 3\}$. It means images can be rotated in four directions and this direction was considered as the output label: $\{L \in \{1, \dots, 4\}\}$. So, this is a 4-class classification task. However, in contrast to conventional approach, our rotation method was performed on each part of an image (Fig 2). This means, each piece of an image would be able to rotate independently from another. So, the main rotation approach converted to four 4-class classification tasks.

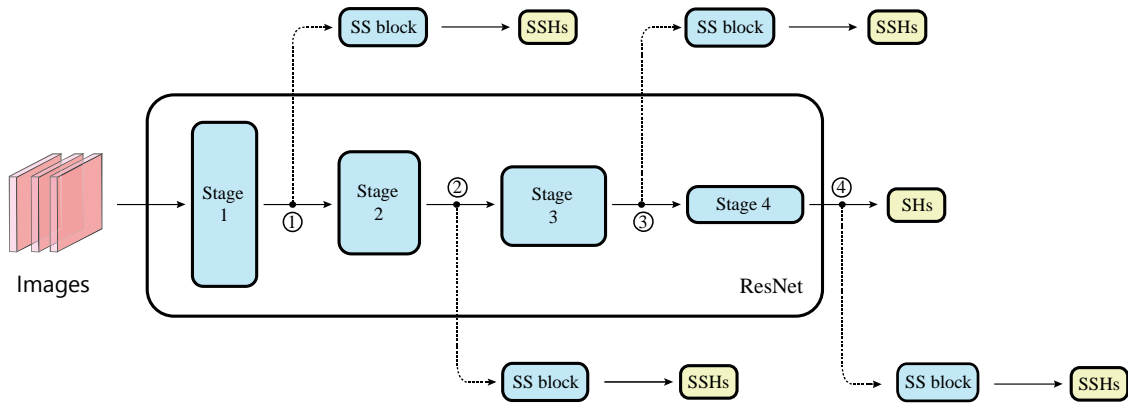


Fig 1 Testing different branches for SHs and SSHs. Every number is a point for Self-Supervised heads separation.

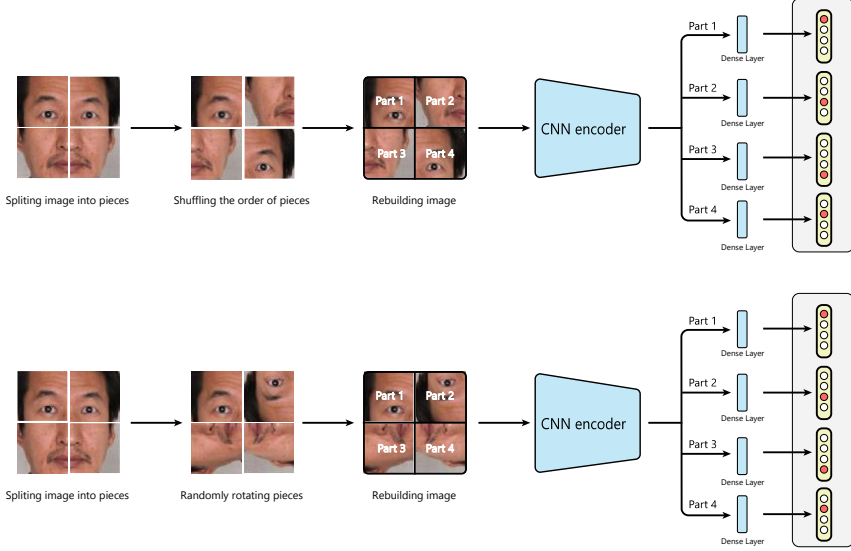


Fig 2 Procedure of Puzzling (upper) and rotation (lower) methods in SSL. Each head describes a local part in the image.

Puzzling-Rotation. The puzzling-rotation approach was based on the combination of puzzles and rotation, and the rotation part performed on each puzzle piece individually. It is also important to know, each region has two tasks. So, for 2×2 puzzling-rotation, eight Self-Supervised tasks were created. But if we rotated all puzzle pieces then, because of the perturbation, the information of Head Pose could be lost. In other words, there could be more than one correct solution for a single sample and this was not good to route Head Pose information through the network. To overcome this issue, we had to rotate at most two puzzle pieces randomly and the rest must be left unchanged. This led to the remaining of main tasks information inside of images. It's obvious that unchanged pieces took zero label for rotation.

We looked through the usage of three approaches on supervised fine-grained Head Pose estimation:

- SS pre-training weights
- ImageNet pre-training weights
- SS auxiliary training (HMTL)

Also, to evaluate our approach, HMTL with ImageNet and SS pre-training weights was done as well. All auxiliary tasks were the classification task, so, all losses were categorical cross entropy. Formula 1 shows MTL loss optimization for puzzling-rotation method in a finding best architecture. Need to mention that HopeNet architecture was not considered in this part.

$$\begin{aligned}
 \mathcal{L}_{total} &= \mathcal{L}_{SL} + \mathcal{L}_{SSL} = (\mathcal{L}_{Yaw} + \mathcal{L}_{Pitch}) \\
 &+ \left(\sum_j \mathcal{L}_{Puzzle_j} + \sum_j \mathcal{L}_{Rotation_j} \right) \\
 &= \left(\sqrt{\frac{1}{n} \sum_{j=1}^n (\hat{y} - y)^2} + \sqrt{\frac{1}{n} \sum_{j=1}^n (\hat{y} - y)^2} \right) + \\
 &\sum_j \left(\sum_i y_{i,j} \log(\hat{y}_{i,j}) + \sum_i y_{i,j} \log(\hat{y}_{i,j}) \right), (1)
 \end{aligned}$$

Where:

- \mathcal{L}_{SL} : two RMSE loss for SHs
- \mathcal{L}_{SSL} : categorical cross entropy for puzzling SSHs and rotation SSHs

4. Results

As we described in the previous section, the ResNet50 architecture was used as the encoder. Inputs of all methods were set to $224 \times 224 \times 3$. To train networks in this paper, $2 \times$ RTX 2070 8GB GPU cards were used. For training all models in this section, an Adabelief optimizer [37] with batch size 64 has been used. Also, mixed precision was used to speed up training. All the experiments were written by the TensorFlow 2 framework in python.

4.1 Finding Multi-task architecture

Here, at first, the original ResNet50 architecture was considered and then, four flags were defined on it in order to divide an SSL branch from that flag. To do this, ETH-XGaze dataset was selected and only Head Pose labels were used. We used ETH-XGaze because it is divided based on subject numbers which could help us to understand generality of methods based on the number of subjects. It just has Yaw and Pitch axis for Head Pose estimation and it did not include the Roll axis. Because of the huge amounts of images in it, one subject from train sets were selected which were about 10,000 samples. We did this because with low amounts of data we could measure the difference clearer. On the other hand, in evaluation step, we separated three subjects from train set as the validation set which were 108, 109 and 111. Moreover, we did random zooms, random hue transformations and Dropout [38] to prevent Overfitting. For SHs and SSHs, Dropout layers with values of 0.4 and 0.2 were used respectively

The SSL's divided branch is a ResNet50's convolution block with skip connection which has three ConvNet layers with Batch Normalization that is shared for both. After a convolution block, for each image zone tasks (rotation and puzzle), a dense layer

followed by a softmax layer is placed. Both the rotation and puzzle pre-text branches are the same. Of course, there are more ways to design and divide SSL branches which we considered for future research. We tried to find the best the branching point of SL+SSL learning for three SSL tasks:

- 2×2 Puzzle
- 2×2 Rotation
- 2×2 Puzzle-Rotation

Need to motioned that in the Puzzle-Rotation, each rotation and puzzle tasks have separate branches but the branching points are the same. Finally, in training iteration, samples in every batch are like $\{(X, Y) = (X, (R_i, P_i); i \in (1, \dots, 4))\}$ for the Puzzle-Rotation, $\{(X, Y) = (X, (P_i); i \in (1, \dots, 4))\}$ for the Puzzle and $\{(X, Y) = (X, (R_i); i \in (1, \dots, 4))\}$ for the Rotation. Results are placed in Table 1 and Fig 3.

We had two supervised heads which belong to Yaw and Pitch labels. Each one was created by a regression Dense layer on top of CNN output. All methods have been trained for 110 epochs. At first, learning rate set to 0.001, and in epoch 30 and 40, it multiplied by 0.1.

It was shown in the result that the number three point has lower errors compared to other points. Based on results, we could see the Yaw error dropped remarkably for puzzling. However, the rotation auxiliary task did not help SHs to reduce the error rate. Consequently, we consider the branching point number three as the architecture for the SL+SSL.

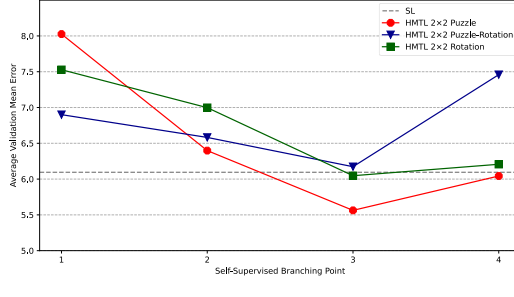


Fig 3 The Average of yaw and pitch Mean error for Different flags with 2×2 puzzling, rotation and puzzling-rotation on ETH-XGaze. It can be seen that HMTL 2×2 puzzle performed better than others at point 3.

Table 1 Results of mean average errors for Yaw and Pitch via different flags.

Method	Flag	Yaw (MAE)	Pitch (MAE)	Average
HMTL puzzling-rotation 2×2	1	5.075	8.725	6.9
HMTL puzzling-rotation 2×2	2	5.243	7.921	6.582
HMTL puzzling-rotation 2×2	3	5.243	7.921	6.582
HMTL puzzling-rotation 2×2	4	5.243	7.921	6.582
HMTL rotation 2×2	1	4.985	10.072	7.528
HMTL rotation 2×2	2	4.373	9.623	6.998
HMTL rotation 2×2	3	4.757	7.337	6.047
HMTL rotation 2×2	4	4.701	7.712	6.207
HMTL puzzling 2×2	1	6.478	9.575	8.026
HMTL puzzling 2×2	2	5.667	7.13	6.398
HMTL puzzling 2×2	3	4.272	6.852	5.563
HMTL puzzling 2×2	4	4.347	7.738	6.043
SL	-	5.338	6.852	6.095

4.2 Self-supervised learning for fine-grained Head Pose estimation

As we mentioned before our goal was analyzing impact of three things on supervised task:

1. SSL pre-training
2. SSL auxiliary task
3. SSL auxiliary task with SSL pre-training

In the previous section we defined proper dividing point for SSL branches and found the best point. In this section, we consider the best architecture (flag point 3) as our proposed architecture. The supervised heads were based on HopeNet with alpha value of 2. Like the original work, we considered 300W-LP [20] for training which consists of synthesize head pose samples. For the validation, AFLW2000 and BIWI were considered.

We trained them for 110 epochs. All learning rates started with 0.001 and at epoch 20 and 100, they multiplied by 0.1. Also, two levels of augmentation were applied. The first level consisted of random central zoom and random contrast, and the second level beside level one transformations, included blurring, down scale resolution and cutout. Moreover, for all supervised and self-supervised heads, Dropout layers with values of 0.5 and 0.2 were used respectively. As the value of supervised losses were much bigger than each SS losses, all loss function of self-supervised heads, puzzling and rotation, were multiplied by 50. Formula 2 showed HMTL puzzling MTL optimization.

$$\begin{aligned}
 \mathcal{L}_{Total} &= \mathcal{L}_{SL} + \mathcal{L}_{SSL} = \mathcal{L}_{Cat-Reg} + \mathcal{L}_{puzzle} \\
 &= \mathcal{L}_{Cat} + \alpha \mathcal{L}_{Reg} + \sum_j \mathcal{L}_{Puzzle_j} \\
 &= \left(- \sum_i y_{Cat_i} \log(\hat{y}_{Cat_i}) + \alpha \sqrt{\frac{1}{n} \sum_{j=1}^n (y_{Reg_j} - E(\hat{y}_{Cat})_j)^2} \right)_{yaw} \\
 &+ \left(- \sum_i y_{Cat_i} \log(\hat{y}_{Cat_i}) + \alpha \sqrt{\frac{1}{n} \sum_{j=1}^n (y_{Reg_j} - E(\hat{y}_{Cat})_j)^2} \right)_{pitch} \\
 &+ \left(- \sum_i y_{Cat_i} \log(\hat{y}_{Cat_i}) + \alpha \sqrt{\frac{1}{n} \sum_{j=1}^n (y_{Reg_j} - E(\hat{y}_{Cat})_j)^2} \right)_{roll} \\
 &+ \sqrt{\frac{1}{n} \sum_{j=1}^n (y_{Reg_j} - E(\hat{y}_{Cat})_j)^2}, (2)
 \end{aligned}$$

Where:

- L_{Cat} : categorical cross entropy for categorical loss
- L_{Reg} : RMSE loss functions for yaw, pitch and roll heads
- \hat{y}_{Cat} : output of softmax layer
- y_{Cat} : true label for categorical loss
- α : weight for the regression losses
- E : expectation of softmax layer after categorical head output to calculate regression value

Table 2 Results of different methods on the AFLW2000. Our SL methods are based on HopeNet architecture. *: indicates that reduced version of AFLW2000 was used. \dagger : indicates that bin size for categorical intervals set to 1. The bin size for the rest is 3. \cap : down sampling transformation to 15X.

Method	Aug	Pre-train weights	Yaw	Pitch	Roll	Average
FAN (12 points) [39]	Unknown	-	18.273	12.604	8.998	13.292
3DDFA [20]	Unknown	-	5.4	8.53	8.250	7.393
RetinaFace R-50 (5 points) [40]	Unknown	-	5.101	9.642	3.924	6.222
HopeNet [7]	≈ 2	-	6.47	6.559	5.436	6.155
Hybrid Coarse-Fine* [41]	Unknown	-	4.82	6.227	5.137	5.395
HPE-40* [10]	Unknown	-	4.87	6.18	4.8	5.28
FSA-Caps-Fusion* [12]	≈ 2	-	4.5	6.08	4.64	5.07
WHENet* [11]	\cap	-	4.44	5.75	4.31	4.83
TriNet* [42]	Unknown	-	4.198	5.767	4.042	4.669
QuatNet [43]	Unknown	-	3.97	5.61	3.92	4.5
Img2pose* [44]	Unknown	-	3.426	5.034	3.278	3.913
SL	1	-	6.679	8.219	7.067	7.322
SL*	1	-	5.736	5.907	4.89	5.511
SL	1	ETH-XGaze SSL 2x2 puzzling	6.437	8	6.703	7.047
SL	1	ETH-XGaze SSL 2x2 rotation	5.921	8.086	7.027	7.011
SL*	1	ETH-XGaze SSL 2x2 rotation	5.86	5.541	4.113	5.171
SL	1	ImageNet	6.001	8.190	6.967	7.053
SL*	1	ImageNet	5.973	5.488	4.191	5.217
SL	2	-	5.278	7.987	6.638	6.634
SL*	2	-	6.221	5.569	3.984	5.258
SL*	2	ETH-XGaze SSL 2x2 rotation	5.355	5.432	4.175	4.987
HMTL 2x2 puzzling	1	-	5.421	8.464	7.081	6.989
HMTL 2x2 puzzling*	1	-	4.22	6.065	5.007	5.094
HMTL 3x3 puzzling	1	-	4.289	8.408	7.009	6.569
HMTL 3x3 puzzling*	1	-	4.175	5.8	4.951	4.975
HMTL 3x3 puzzling	1	ETH-XGaze SSL 2x2 puzzling	4.396	8.402	7.009	6.602
HMTL 3x3 puzzling	1	ETH-XGaze SSL 2x2 rotation	4.223	8.38	6.839	6.48
HMTL 3x3 puzzling*	1	ETH-XGaze SSL 2x2 rotation	3.855	6.065	4.377	4.766
HMTL 3x3 puzzling	1	ImageNet	4.507	8.344	6.773	6.541
HMTL 3x3 puzzling*	1	ImageNet	4.235	6.2	4.231	4.889
HMTL 3x3 puzzling	2	-	3.742	7.796	6.496	6.011
HMTL 3x3 puzzling*	2	-	3.874	5.929	4.416	4.74
HMTL 3x3 puzzling*	2	-	3.967	5.942	4.191	4.7
HMTL 3x3 puzzling*	2	ETH-XGaze SSL 2x2 rotation	3.682	5.919	4.316	4.639
HMTL 2x2 rotation	1	-	6.96	8.221	7.2	7.461
HMTL 2x2 rotation*	1	-	5.998	5.604	4.31	5.304
HMTL 2x2 rotation	1	ETH-XGaze SSL 2x2 puzzling	6.63	7.961	6.92	7.17
HMTL 2x2 rotation*	1	ETH-XGaze SSL 2x2 puzzling	5.77	5.657	4.104	5.177
HMTL 2x2 puzzling-rotation	1	-	5.13	8.553	7.41	7.031
HMTL 2x2 puzzling-rotation*	1	-	5.554	6.211	5.312	5.692

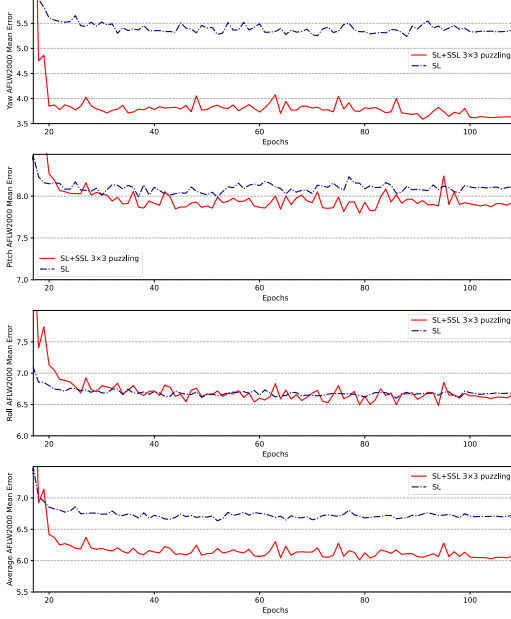


Fig 4 Comparing yaw, pitch and roll validation errors for SL and HMTL on AFLW2000 at different epochs. The SL is HopeNet method. Augmentation level was level 2. The AFLW2000 was used w/o removing any samples.

Table 3 Results of different methods on the BIWI. The SL methods are HopeNet that we implemented. All of our method used level two augmentation and the bin size for categorical intervals set to 1.

Method	Pre-train weights	Yaw	Pitch	Roll	Avg
HopeNet [7]	-	4.810	6.606	3.269	4.895
QuatNet [43]	-	4.01	5.49	2.93	4.14
FSA-Caps-Fusion [12]	-	4.27	4.96	2.76	4.0
WHENet [11]	-	3.60	4.10	2.73	3.48
SL	-	4.322	5.94	3.113	4.458
SL	ImageNet	4.379	5.636	3.002	4.339
SL	ETH-XGaze SSL 2x2 rotation	4.298	5.891	2.782	4.323
HMTL 2x2 rotation	-	4.356	5.801	3.27	4.476
HMTL 3x3 puzzling	-	4.123	5.317	3.059	4.166
HMTL 3x3 puzzling	ImageNet	3.988	4.952	3.01	3.983
HMTL 3x3 puzzling	ETH-XGaze SSL 2x2 rotation	3.864	4.641	2.962	3.822

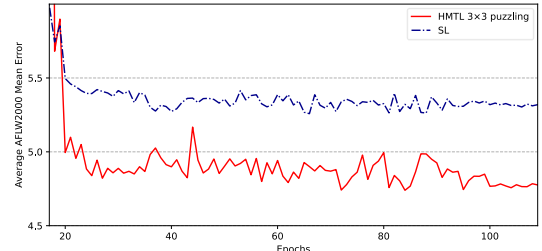


Fig 5 Comparing average MAE for SL and HMTL on the reduced version of AFLW2000 at different epochs. The SL method is HopeNet. Augmentation level was level 2.

The important point for pre-training is that SSL pre-training has performed on the encoder (ResNet50). Results are shown in Table 2 and 3. At first, in contrast to baseline method (HopeNet), we did not remove the samples with absolute value larger than 99 degrees from AFLW2000. There were 31 samples included. We thought, that could be one of the reasons for the difference between our methods with other works in error rate. Thus, we also showed the best proposed method with the reduced version of AFLW2000 (without the 31 samples) to compare it with other methods fairly. Furthermore, we set the bin size for categorical tasks to both 3 and 1 degree. From results, we observed how auxiliary SSL tasks could reduce the average error rate significantly (Fig 4). But, in contrast to puzzling, the rotation auxiliary was not better than SL.

4.3 Barlow Twins pre-training

For a comparison, we tried to implement Barlow Twins [25] (BT) SSL technique for Head Pose estimation. As far as we were concerned, BT was one the best SSL methods which was easy to implement compared to other methods such as DINO [14], BYOL [13], SimCLR [24]. Also, BT works well with CNN backbones which means it is relatively cheap to train.

In order to train ResNet50 with BT, we chose the train set of ETH-XGaze dataset which means there were approximately 0.75 million images. Since BT does not need any negative pairs, each image was transformed twice to create two distorted views. To be precise, an image at first rotated randomly in $\{0, 90, 180, 270\}$ degrees and then the two transformations were performed. The transformations included random cropping, color jittering, converting to grayscale, random Gaussian noise, Gaussian blurring, cutout and random resizing. Random cropping and random Gaussian noise were applied always, though color jittering and converting to grayscale were applied randomly with 0.8 and 0.3 probability. Then one of the blurring and resizing selected randomly and each one could be applied with 0.2 probability. Finally, cutout was performed on each image separately. Except above transformations, we did pre-training one more time with random 3×3 puzzling transformation before performing cutout.

Table 4 Results of BT and HMTL on the reduced version of AFLW2000. Encoder pre-training was performed on the ETH-XGaze images. All training were done with level 2 augmentation and the same settings. HMTL refers to HMTL 3 \times 3 puzzling. The LE and FT refer to linear evaluation and fine-tuning respectively. *: indicates that pre-training with random 3 \times 3 puzzling transformation was used.

Method	Encoder pre-training	Yaw (MAE)	Pitch (MAE)	Roll (MAE)	Avg
HopeNet [7]	-	6.221	5.569	3.984	5.258
HopeNet [7] (LE)	2 \times 2 Rotation	17.198	11.694	11.775	13.556
HopeNet [7] (LE)	2 \times 2 Puzzling	17.408	11.453	11.465	13.442
HopeNet [7] (LE)	3 \times 3 Puzzling	14.509	11.132	10.657	12.099
HopeNet [7] (LE)	BT [25]	9.1	11.753	10.820	10.558
HopeNet [7] (LE)	BT* [25]	10.136	9.477	9.873	9.799
HopeNet [7] (FT)	BT [25]	4.790	5.34	3.677	4.603
HopeNet [7] (FT)	BT* [25]	4.56	5.289	3.596	4.481
HMTL	-	3.874	5.929	4.416	4.74
HMTL (FT)	BT [25]	3.406	5.718	4.103	4.409
HMTL (FT)	BT* [25]	3.351	5.633	3.829	4.271

Like the original work, the encoder contained a ResNet-50 network followed by a projector head. The projector network has three linear layers, each with 2048 output units. The first two layers of the projector were followed by a batch normalization layer and rectified linear units. The encoder trained with batch

size of 64 for 64 epochs and the learning rate was 0.001 with cosine decay. Next, the ResNet encoder used for linear evaluation and fine-tuning on the 300W-LP dataset. All fine-tuning started with 5 epochs of warmup. The results are shown on the table 4. Based on the results, HMTL with BT weights had lower average MAE compared to the vanilla fine-tuning on the HopeNet.

5. Ablation study

5.1 Impact of Self-Supervised heads on Supervised heads

A work [12] showed that local features are important for Pose estimation. Proposed method handles input as a bag of features from an image and ignores the spatial relationship in the feature map. In other words, it says that local spatial features are quite useful to estimate fine-grained pose estimation. By the way, we encountered a question: how much the local and global spatial features are important for Head Pose problem?

We tried to find out the answer via doing an ablation test. In fact, we investigated impact of SSHs on the main Supervised task. At first, a simple SL method trained with puzzled images (HMTL w/o SSHs), then compare it with HMTL via same settings of section 4.2. Fig 5, 6 compared the AFLW2000 error rate on different epochs and numbers are placed in Table 5. We observed that puzzled images did better compared to normal images and was placed in between SL and HMTL in terms of average error rate.

Table 5 Results of ablation study on the reduced version of AFLW2000. The SL and HMTL w/o SSHs methods are HopeNet. All training were done with the same settings.

Method	Yaw (MAE)	Pitch (MAE)	Roll (MAE)	Avg
SL	6.221	5.569	3.984	5.258
HMTL 3 \times 3 puzzling w/o SSHs	4.589	6.223	4.465	5.092
HMTL 3 \times 3 puzzling	3.874	5.929	4.416	4.74

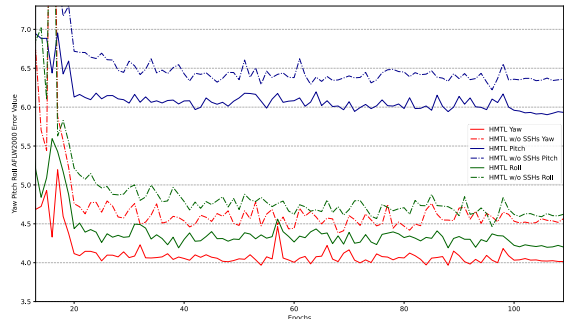


Fig 6 Error rate of HMTL and HMTL w/o SSHs methods on the reduced versions of AFLW2000. HMTL w/o SSHs is HopeNet method which was fed puzzled images. Both methods were trained under same settings: learning rate, learning rate decay schedule, regularization, augmentation level.

5.2 HMTL on limited subjects

In this section, the impact of adding SS auxiliary tasks on supervised task based on the limited number of subjects was examined. In order to do this, ETH-XGaze dataset was picked and only Head Pose labels were used. It has 80 subjects in train set. Like section 4.1, we separated three subjects as validation

set which were 108, 109 and 111. Here, we tried to show the effect of auxiliary tasks on data sizes compared to SL alone.

For SL, ResNet50 was selected, also, by considering the possibility of Categorical-Regression impact on the ablation, we only used regression head on top of the backbone for SHs (Formula 3). For SL+SSL, extended ResNet50 which was defined in section 4.1 was selected. SHs is considered as the best version of table 1 (3×3 puzzling) in section 4.1. Also, beside those, we feed SL with SL+SSL inputs to evaluate images perturbation's effect, like puzzling, on Head Pose estimation. For all three approaches we initialized the ResNet50 with identical random weights seed.

Random central zoom, random gaussian noise, cutout, random hue, random brightness and contrast transformation were used to augment input images heavily. Results are placed on Table 6 and visualized in Fig 7. We found that despite feeding puzzled images into supervised HopeNet architecture had beneficial effect, when simple regression heads were used, it had a negative consequence on the average MAE.

$$\begin{aligned} \mathcal{L}_{Total} &= \mathcal{L}_{SL} + \mathcal{L}_{SSL} = (\mathcal{L}_{Yaw} + \mathcal{L}_{Pitch}) + \sum_j \mathcal{L}_{Puzzle_j} \\ &= \left(\sqrt{\frac{1}{n} \sum_{j=1}^n (\hat{y} - y)^2} + \sqrt{\frac{1}{n} \sum_{j=1}^n (\hat{y} - y)^2} \right) \\ &\quad + \sum_j \sum_i y_{i,j} \log(\hat{y}_{i,j}), \quad (3) \end{aligned}$$

Where:

- \mathcal{L}_{SL} : two RMSE loss for supervised heads
- \mathcal{L}_{SSL} : categorical cross entropy for every puzzling self-supervised heads

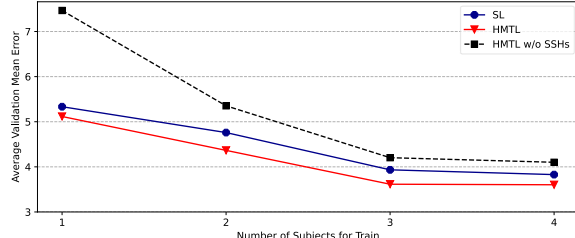


Fig 7 Mean average of yaw and pitch errors for Different number of subjects.

Table 6 Results of mean average errors for Yaw and Pitch via different subjects. Results of this table are the same with Fig 7.

Method	Subjects	Yaw (MAE)	Pitch (MAE)	Avg
SL	1	4.618	6.048	5.333
SL	2	4.69	4.83	4.76
SL	3	3.738	4.130	3.934
SL	4	3.264	4.392	3.828
HMTL 2x2 puzzling	1	3.739	6.493	5.116
HMTL 2x2 puzzling	2	3.495	5.235	4.365
HMTL 2x2 puzzling	3	3.023	4.207	3.615
HMTL 2x2 puzzling	4	3.12	4.086	3.603
HMTL 2x2 puzzling w/o SSHs	1	6.6	8.332	7.466
HMTL 2x2 puzzling w/o SSHs	2	4.746	5.96	5.353
HMTL 2x2 puzzling w/o SSHs	3	3.490	4.916	4.203
HMTL 2x2 puzzling w/o SSHs	4	3.705	4.498	4.101

6. Discussion

In this article, we tried to answer two questions:

- **How SSL can be utilized for fine-grained Head Pose estimation?**
- **How architecture design can impact on fine-grained Head Pose estimation when adding Self-Supervised auxiliary task?**

For the first question, we showed that there are mainly two ways to use SSL: Pre-training it for fine-tuning or using SS as auxiliary tasks besides SL tasks. Both methods can reduce error rates but the latter shows better results.

From another view, when we use SS auxiliary, the branching point for heads are very important. Previous studies [17], [19] has shown the effectiveness of MTL. It was shown that some heads could help each other while others may hurt one another. We did not know how to exactly find the correlation of tasks and we can just find it practically. Due to the fact that our computation budget was limited, we could not go for Neural Architecture Search (NAS) which was pretty expensive. So, four points were defined as shared representation locations and after those points, SHs from SSHs were separated. Testing different points approximately showed us the best point for dividing heads. We did this via two SS pre-text heads, puzzling and rotation. Results indicated that using SSL auxiliary was effectiveness than ImageNet pre-training but only by one of SSL pre-text tasks. Indeed, the other one (rotation) even slightly hurt the supervised error rates. Even though the rotation Self-Supervision could not be as effective as an auxiliary task, it was surprisingly helpful to be used as a pre-training technique. Furthermore, an interesting point we found was the effect of puzzled images alone on error reduction via SL. In fact, both puzzled images and adding auxiliary tasks help each other to reduce the average error. Moreover, it was not limited to large amount of data and HMTL could also be effective for low data regime as they showed for FER [19]. Our hybrid approach only has applied for training stage and in the evaluation time or test time, all SS branches could be removed from the main encoder. This means that there is no change in supervised architecture and the inference time of production environments respectively.

Though, we encountered with many questions in this paper which can be considered for future research:

1. Which architecture is best for Self-Supervised auxiliary tasks?

Even though, we could show the impact of different branching point on SHs error rate, there is much vagueness about which architecture should be used for each SS tasks and which task hurt Supervised tasks instead of helping them (negative transfer). We think, this issue can be explored by NAS for the best architecture design and Gradient Modulation [45] for conflicting task gradients.

2. How to deal with different losses in HMTL optimization?

Different tasks in the MTL approach mean different losses. e.g., regression and classification losses are not similar in values, learning speed and performance [45]. When a model is to be

trained on more than one task, the various task-specific loss functions must be merged into a single aggregated loss function which the neural network is trained to minimize. The simplest method, manual loss weighting, was used in this paper, but there are more promising methods like Geometric Mean of Losses [46] and weighting by uncertainty [47] that has the potential to improve results and to prohibit training collapses for different tasks.

3. How to find the best SSL auxiliary task for helping a supervised task like Head Pose estimation?

Actually, we don't exactly know but, by recent progress in SSL methods, we think, adding auxiliary task of new approaches to the SL is feasible and are more powerful than pretext tasks, specifically, a non-contrastive method which does not need negative pairs while training [14], [25]. This paper indicated that Barlow Twins pre-training weights reduced the average error rate in HMTL architecture more than vanilla supervised fine-tuning. Furthermore, we guess the representation of best SSL methods, like non-contrastive methods, have higher and more abstract feature levels than SL representation because of generalization of SSL approaches, as we saw in DINO [14]. Indeed, in this training setting, SHs can act as auxiliary tasks for SS representation learning. However, finding or designing methods like Self-Supervised pre-text tasks are easier and cheaper to pursue and sometime could lead to magnificent result [48].

7. Conclusion

In this article, we tried to show how SSL could be used for Fine-grained Head Pose estimation. We showed there are two ways to do that, using SSL as a pre-train feature extractor or using it as an auxiliary task besides the main task which the second approach indicated lower average error compared to the first one.

We built an architecture based on ResNet50 by connecting SSL heads to it, called HMTL. In order to connect SS branches to the main encoder (ResNet50), three branching points were considered and then, we found the best point to created our hybrid architecture. Results showed that the combination of both approaches were the best. In other words, by applying SSH pre-trained features as initializer of backbone and adding auxiliary task during training, the average MAE reduced to 23.1% and 13% with and without additional dataset respectively compared to the baseline (HopeNet) which were comparable to the state-of-the-art methods. Also, we found that the puzzling task was good as an auxiliary task and the rotation task was only decent as a pre-training technique. Finally, we showed that our method was also good when the number of subjects was restricted.

Acknowledgments

We gratefully acknowledge Hadi Pourmirzaei, Mohammad Pourmirzaei and Elahe Ghazalifar for preparing pictures, resource preparation and helpful discussions.

References

- [1] D. Gerónimo, A. M. López, A. D. Sappa, and T. Graf, "Survey of pedestrian detection for advanced driver assistance systems," *IEEE Trans. Pattern Anal. Mach. Intell.*, 2010, doi: 10.1109/TPAMI.2009.122.
- [2] Z. Chen *et al.*, "A realistic face-to-face conversation system based on deep neural networks," 2019, doi: 10.1109/ICCVW.2019.00315.
- [3] Z. Liu, H. Hu, Z. Wang, K. Wang, J. Bai, and S. Lian, "Video synthesis of human upper body with realistic face," 2019, doi: 10.1109/ISMAR-Adjunct.2019.00-47.
- [4] S. S. Mukherjee and N. M. Robertson, "Deep Head Pose: Gaze-Direction Estimation in Multimodal Video," *IEEE Trans. Multimed.*, 2015, doi: 10.1109/TMM.2015.2482819.
- [5] K. Cao, Y. Rong, C. Li, X. Tang, and C. C. Loy, "Pose-Robust Face Recognition via Deep Residual Equivariant Mapping," 2018, doi: 10.1109/CVPR.2018.00544.
- [6] Z. Liu, Z. Chen, J. Bai, S. Li, and S. Lian, "Facial pose estimation by deep learning from label distributions," 2019, doi: 10.1109/ICCVW.2019.00156.
- [7] N. Ruiz, E. Chong, and J. M. Rehg, "Fine-grained head pose estimation without keypoints," 2018, doi: 10.1109/CVPRW.2018.00281.
- [8] R. Valle, J. M. Buenaposada, and L. Baumela, "Multi-Task Head Pose Estimation in-the-Wild," *IEEE Trans. Pattern Anal. Mach. Intell.*, 2021, doi: 10.1109/TPAMI.2020.3046323.
- [9] A. Sheka and V. Samun, "Knowledge Distillation from Ensemble of Offsets for Head Pose Estimation," Aug. 2021, Accessed: Oct. 01, 2021. [Online]. Available: <http://arxiv.org/abs/2108.09183>.
- [10] B. Huang, R. Chen, W. Xu, and Q. Zhou, "Improving head pose estimation using two-stage ensembles with top-k regression," *Image Vis. Comput.*, 2020, doi: 10.1016/j.imavis.2019.11.005.
- [11] Y. Zhou and J. Gregson, "WHENet: Real-time Fine-Grained Estimation for Wide Range Head Pose," May 2020, Accessed: Aug. 08, 2021. [Online]. Available: <https://arxiv.org/abs/2005.10353>.
- [12] T. Y. Yang, Y. T. Chen, Y. Y. Lin, and Y. Y. Chuang, "Fsa-net: Learning fine-grained structure aggregation for head pose estimation from a single image," 2019, doi: 10.1109/CVPR.2019.00118.
- [13] J. B. Grill *et al.*, "Bootstrap your own latent a new approach to self-supervised learning," 2020.
- [14] M. Caron *et al.*, "Emerging Properties in Self-Supervised Vision Transformers," Apr. 2021, Accessed: Aug. 08, 2021. [Online]. Available: <https://arxiv.org/abs/2104.14294>.
- [15] X. Chen and K. He, "Exploring Simple Siamese Representation Learning," Nov. 2020, Accessed: Aug. 09, 2021. [Online]. Available: <https://arxiv.org/abs/2011.10566v1>.
- [16] Y. M. Asano, C. Rupprecht, and A. Vedaldi, "A critical analysis of self-supervision, or what we can learn from a single image," Apr. 2019, Accessed: Aug. 08, 2021. [Online]. Available: <https://arxiv.org/abs/1904.13132>.
- [17] T. Stendley, A. Zamir, D. Chen, L. Guibas, J. Malik, and S. Savarese, "Which tasks should be learned together in multi-task learning?," 2020.
- [18] M. Crawshaw, "Multi-Task Learning with Deep Neural Networks: A Survey," Sep. 2020, Accessed: Aug. 08, 2021. [Online]. Available: <https://arxiv.org/abs/2009.09796>.
- [19] M. Pourmirzaei, G. A. Montazer, and F. Esmaili, "Using Self-Supervised Auxiliary Tasks to Improve Fine-Grained Facial Representation," May 2021, Accessed: Aug. 30, 2021. [Online]. Available: <http://arxiv.org/abs/2105.06421>.
- [20] X. Zhu, Z. Lei, X. Liu, H. Shi, and S. Z. Li, "Face alignment across large poses: A 3D solution," 2016, doi: 10.1109/CVPR.2016.23.
- [21] X. Yin, X. Yu, K. Sohn, X. Liu, and M. Chandraker, "Towards Large-Pose Face Frontalization in the Wild," 2017, doi: 10.1109/ICCV.2017.430.
- [22] G. Fanelli, M. Dantone, J. Gall, A. Fossati, and L. Van Gool, "Random Forests for Real Time 3D Face Analysis," *Int. J. Comput. Vis.*, 2013, doi: 10.1007/s11263-012-0549-0.
- [23] X. Zhang, S. Park, T. Beeler, D. Bradley, S. Tang, and O. Hilliges, "ETH-XGaze: A Large Scale Dataset for Gaze Estimation Under Extreme Head Pose and Gaze Variation," 2020, doi: 10.1007/978-3-030-58558-7_22.
- [24] T. Chen, S. Kornblith, K. Swersky, M. Norouzi, and G. Hinton, "Big Self-Supervised Models are Strong Semi-Supervised

Learners,” *arXiv*. 2020.

[25] J. Zbontar, L. Jing, I. Misra, Y. LeCun, and S. Deny, “Barlow Twins: Self-Supervised Learning via Redundancy Reduction,” *arXiv Prepr. arXiv2103.03230*, 2021.

[26] E. Cole, X. Yang, K. Wilber, O. Mac Aodha, and S. Belongie, “When Does Contrastive Visual Representation Learning Work?”, May 2021, Accessed: Aug. 08, 2021. [Online]. Available: <https://arxiv.org/abs/2105.05837>.

[27] D. Wu *et al.*, “Align Yourself: Self-supervised Pre-training for Fine-grained Recognition via Saliency Alignment,” Jun. 2021, Accessed: Aug. 08, 2021. [Online]. Available: <http://arxiv.org/abs/2106.15788>.

[28] S. K. Mustikovela *et al.*, “Self-Supervised Viewpoint Learning from Image Collections,” 2020, doi: 10.1109/CVPR42600.2020.00403.

[29] J. N. Kundu, S. Seth, V. Jampani, M. Rakesh, R. Venkatesh Babu, and A. Chakraborty, “Self-supervised 3D human pose estimation via part guided novel image synthesis,” 2020, doi: 10.1109/CVPR42600.2020.00619.

[30] K. Yun, J. Park, and J. Cho, “Robust Human Pose Estimation for Rotation via Self-Supervised Learning,” *IEEE Access*, 2020, doi: 10.1109/ACCESS.2020.2973390.

[31] A. Dahiyta, A. Spuri, and O. Hilliges, “Exploring self-supervised learning techniques for hand pose estimation,” in *NeurIPS 2020 Workshop on Pre-registration in Machine Learning*, 2021, vol. 148, pp. 255–271, [Online]. Available: <https://proceedings.mlr.press/v148/dahiyta21a.html>.

[32] X. Zhai, A. Oliver, A. Kolesnikov, and L. Beyer, “S4L: Self-Supervised Semi-Supervised Learning,” May 2019, Accessed: Aug. 08, 2021. [Online]. Available: <http://arxiv.org/abs/1905.03670>.

[33] B. Korbar, D. Tran, and L. Torresani, “Cooperative Learning of Audio and Video Models from Self-Supervised Synchronization,” Jun. 2018, Accessed: Aug. 08, 2021. [Online]. Available: <http://arxiv.org/abs/1807.00230>.

[34] T. Han, W. Xie, and A. Zisserman, “Self-supervised Co-training for Video Representation Learning,” Oct. 2020, Accessed: Aug. 08, 2021. [Online]. Available: <https://arxiv.org/abs/2010.09709>.

[35] K. He, X. Zhang, S. Ren, and J. Sun, “Deep residual learning for image recognition,” 2016, doi: 10.1109/CVPR.2016.90.

[36] S. Gidaris, P. Singh, and N. Komodakis, “Unsupervised representation learning by predicting image rotations,” *arXiv*. 2018.

[37] J. Zhuang *et al.*, “AdaBelief optimizer: Adapting stepsizes by the belief in observed gradients,” *arXiv*. 2020.

[38] N. Srivastava, G. Hinton, A. Krizhevsky, I. Sutskever, and R. Salakhutdinov, “Dropout: A simple way to prevent neural networks from overfitting,” *J. Mach. Learn. Res.*, 2014.

[39] V. Kazemi and J. Sullivan, “One millisecond face alignment with an ensemble of regression trees,” 2014, doi: 10.1109/CVPR.2014.241.

[40] J. Deng, J. Guo, E. Ververas, I. Kotsia, and S. Zafeiriou, “Retinaface: Single-shot multi-level face localisation in the wild,” 2020, doi: 10.1109/CVPR42600.2020.00525.

[41] H. Wang, Z. Chen, and Y. Zhou, “Hybrid coarse-fine classification for head pose estimation,” *arXiv Prepr. arXiv1901.06778*, 2019.

[42] Z. Cao, Z. Chu, D. Liu, and Y. Chen, “A vector-based representation to enhance head pose estimation,” 2021, doi: 10.1109/WACV48630.2021.00123.

[43] H. W. Hsu, T. Y. Wu, S. Wan, W. H. Wong, and C. Y. Lee, “Quatnet: Quaternion-based head pose estimation with multiregression loss,” *IEEE Trans. Multimed.*, 2019, doi: 10.1109/TMM.2018.2866770.

[44] V. Albiero, X. Chen, X. Yin, G. Pang, and T. Hassner, “img2pose: Face alignment and detection via 6dof, face pose estimation,” in *Proceedings of the IEEE/CVF Conference on Computer Vision and Pattern Recognition*, 2021, pp. 7617–7627.

[45] M. Crawshaw, “Multi-task learning with deep neural networks: A survey,” *arXiv*. 2020.

[46] S. Chemupati, G. Sistu, S. Yogamani, and S. A. Rawashdeh, “MultiNet++: Multi-stream feature aggregation and geometric loss strategy for multi-task learning,” 2019, doi: 10.1109/CVPRW.2019.00159.

[47] R. Cipolla, Y. Gal, and A. Kendall, “Multi-task Learning Using Uncertainty to Weigh Losses for Scene Geometry and Semantics,” 2018, doi: 10.1109/CVPR.2018.00781.

[48] H. Bao, L. Dong, and F. Wei, “BEiT: BERT Pre-Training of Image Transformers,” *arXiv Prepr. arXiv2106.08254*, 2021.